Finite-Element Calculation of Meissner Currents in Multiply Connected Superconductors

Christophe Cordier, Stéphane Flament, and Christian Dubuc

***Abstract*—A three-dimensional (3D) finite-element formulation for calculating Meissner currents in multiply connected superconductors is presented. The fluxoid quantization condition is ensured as simply as possible. The problem is formulated so that we have to solve two systems of equations by the use of a conjugate gradient algorithm without preconditioning. Meissner currents and magnetic-flux density are numerically evaluated in a superconducting tube and around a vortex. These results are compared with analytical solutions.**

***Index Terms*— Finite-element method, modeling, simulation, superconductor, quantization.**

I. Introduction

In order to improve the performances of our superconducting magnetometers we have chosen to optimize the design of these devices. One way to reach this objective is to calculate supercurrents by means of the finite-element method (FEM).

We have given in a preliminary paper a three–dimensional (3D) finite-element formulation for calculating Meissner currents in superconductors [1], however, this formulation only allows us to simulate multiply connected regions provided that the fluxoid is equal to zero. For magnetometers including a superconducting coil, such as SQUID (Superconducting Quantum Interference Device), this limitation is very restrictive. We propose in this paper a method to surmount this restriction.

II. Fluxoid Quantization

The topology of our problem is depicted in Fig. 1. It consists of a multiply connected superconducting region Ω_1 surrounded by a nonsuperconducting region Ω_2 which may contain forced currents.

By writing the macroscopic complex wavefunction of the Cooper pairs in the Schrdinger's equation [2], we find the supercurrent density J_s flowing in Ω_1

$$J_s = \frac{1}{\mu_0 \lambda_L^2}\left(-A + \frac{\Phi_0}{2\pi}\nabla\varphi\right) \tag{1}$$

where $\lambda_L, \Phi_0, \varphi$, and A stand for the London penetration depth, the flux quantum, the phase of the wavefunction, and the magnetic vector potential A, respectively.

Manuscript received July 23, 1999.

The authors are with GREYC-CNRS UPRES A 6072-ISMRA, Université de Caen 6, 14032 Caen Cedex, France (e-mail: ccordier@greyc.ismra.fr).

Publisher Item Identifier S 1051-8223(99)10402-0.

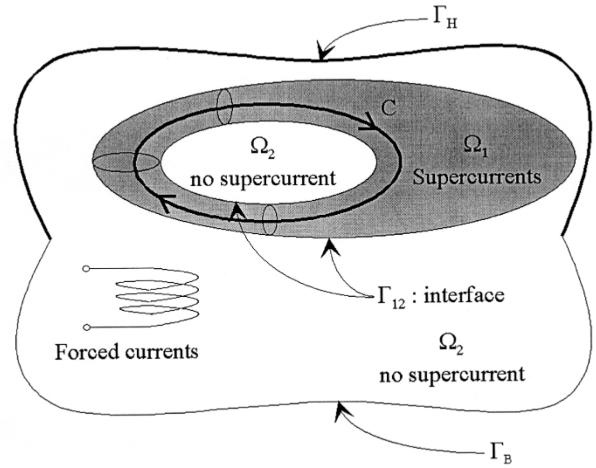

Fig. 1. Topological description of a multiply connected supercurrent problem.

If we integrate (1) on a path C enclosing a nonsuperconducting hole, we obtain the fluxoid

$$\oint_C \mu_0 \lambda_L^2 j_S \cdot dl + \oint_C A \cdot dl = \frac{\Phi_0}{2\pi}\oint_C \nabla\varphi \cdot dl = k\Phi_0. \tag{2}$$

The usual explanation of the second equality (see [2]–[4]) lies in the fact that φ is a phase which is specified modulo 2π

$$\oint_C \nabla\varphi \cdot dl = \lim_{M\to M}[\varphi(M) - \varphi(M')] = 2k\pi \tag{3}$$

where M and M' are two points of the path C.

In this case, calculating J_s is rather complicated as φ is a multivalued variable. The way followed in this paper consists in restricting the variation domain of φ on a single period 2π and in adding a new variable to ensure the fluxoid quantization. In other words, we consider now a single-valued phase which will be called θ and we formulate the physical problem to an equivalent form convenient for the FEM.

The number of flux quanta, trapped in a multiply connected superconductor depends on the magnetic flux density B in the hole at the moment of the superconducting transition. So we consider in our calculation magnetic flux changes before and after this transition. With the usual set of symbols we write the first London equation and the Maxwell–Faraday equation

$$E = \frac{\partial}{\partial t}(\mu_0 \lambda_L^2 J_S) \tag{4}$$

$$\nabla \times E = \frac{\partial B}{\partial t}. \tag{5}$$

Writing (4) in (5) and permuting the time and space differentials gives

$$\nabla \times \left[\frac{\partial}{\partial t}(\mu_0 \lambda_L^2 J_S)\right] = -\frac{\partial B}{\partial t}. \quad (6)$$

By integrating (6) between $t = 0$ and t, respectively, the moment of the superconducting transition and the one following, we get

$$\nabla \times [\mu_0 \lambda_L^2 J_S] + B = (\nabla \times [\mu_0 \lambda_L^2 J_S] + B)_0 = B_Q \quad (7)$$

where index 0 refers to time $t = 0$.

In (7), the term $(\nabla \times [\mu_0 \lambda_L^2 J_S] + B)_0$ is an integration constant which is usually taken equal to zero without any particular reason [5]. From now, this constant which has dimension of a magnetic flux density is called B_Q. We introduce a magnetic vector potential A_Q defined $B_Q = \nabla \times A_Q$. Knowing that the curl of a gradient is null, (7) is therefore equivalent to

$$\nabla \times [\mu_0 \lambda_L^2 J_S + A - A_Q] = \nabla \times \left(\frac{\Phi_0}{2\pi} \nabla \theta\right). \quad (8)$$

From (8) we find the supercurrent density

$$J_s = \frac{1}{\mu_0 \lambda_L^2}\left(-A + \frac{\Phi_0}{2\pi}\nabla\theta + A_Q\right). \quad (9)$$

The fluxoid can then be written

$$\oint_C \mu_0 \lambda_L^2 J_S \cdot dl + \oint_C A \cdot dl = \frac{\Phi_0}{2\pi}\oint_C \nabla\theta \cdot dl + \oint_C A_Q \cdot dl = k\Phi_0. \quad (10)$$

Considering that θ is a single-valued variable, we see that the fluxoid quantization condition can be reduced to

$$\oint_C A_Q \cdot dl = k\Phi_0. \quad (11)$$

This last equation is valid for every path C enclosing the hole, so by using the Stokes theorem, B_Q must be equal to zero in Ω_1 and must verify on every section S spanning the contour C

$$\iint_S B_Q \cdot dS = k\Phi_0. \quad (12)$$

Two remarks follow.

First, the new variable A_Q previously introduced for ensuring the fluxoid quantization, is not physically meaningless since (12) shows that B_Q is a magnetic flux density present in the hole at the transition. A drawback is that we are not able to calculate how many fluxoid quanta are trapped, we must fix their number. This number is usually chosen as the ratio of the applied flux in the hole to the flux quantum.

Second, as B_Q is null in the superconducting region, the curl of (9) also gives the second London equation

$$\nabla \times (\mu_0 \lambda_L^2 J_S) = -B. \quad (13)$$

III. Finite-Element Formulation and Discretization

Our aim is to precisely calculate B and J_s with the nodal FEM. We consider the quasi-stationary state and thus we write the Maxwell–Ampere equation as follows:

$$\nabla \times B = \mu_0 J. \quad (14)$$

The way previously chosen in [1] consists of finding A and θ as solution of a system of equations built from (14). We distinguish two different manners to take into account the fluxoid quantization. These two methods lead to a solution of another system of equations coupled to the first one. The first method consists of writing J_s with (9). In this case, we must determine the vector potential A_Q to completely describe J_s; whereas with the second method, we just have to solve for a scalar potential to describe the fluxoid whatever its value. We will detail this last one as it reduces the computational work.

As it is shown on Fig. 1, the union of Ω_1 and Ω_2 forms the whole space. We distinguish three types of boundaries.

- Γ_B, where the normal component of flux density is equal to zero.
- Γ_H, where the tangential component of magnetic field is set to H_{est}.
- Γ_{12}, the interface between Γ_1 and Γ_2 where flux density is continuous and the normal component of supercurrent is null.

The method presented in this paper lies in the variable change $A^* = A - A_Q$, thus we can write (9) to a useful form equivalent to (1)

$$J_s = \frac{1}{\mu_0 \lambda_L^2}\left(-A^* + \frac{\Phi_0}{2\pi}\nabla\theta\right). \quad 15)$$

By applying this change in (14) we see that we do not need to know A_Q. The knowledge of B_Q is sufficient to describe our problem. We know from (7) that B_Q is free of divergence as the divergence of $\nabla \times J_S$ and B is null. Notice that there are different distributions of B_Q which ensure the fluxoid quantization condition (12). For the sake of simplicity we have built an irrotational B_Q. Therefore, by defining B_Q as a gradient of a scalar potential Ψ, B_Q can be obtained by solving the following system of equations:

$$\nabla \cdot \nabla \Psi = 0, \qquad \text{in } \Omega_2 \quad (16)$$

$$\nabla \Psi \cdot n = 0, \qquad \text{on } \Gamma_{12} \text{ and } \Gamma_B \quad (17)$$

where n is the unit vector normal to the boundary.

To impose the condition (12), we just have to fix the flux of B_Q on an arbitrary section S_a by

$$\nabla \Psi \cdot n = B_{QS}, \qquad \text{on } S_a. \quad (18)$$

We get the uniqueness of Ψ and consequently the one of B_Q by giving a value of Ψ at any point in Ω_2. By analogy with our precedent work [1], the second system of equation, derived from (14), is shown on the top of the following page in (19)–(29), where n is the outer normal on the corresponding surface and indices 1 and 2 refer, respectively, to quantities in regions Ω_1 and Ω_2. The uniqueness of A^* is obtained by enforcing the gauge $\nabla \cdot A^* = 0$ thanks to the term

$$\left.\begin{aligned} &\nabla\times\nabla\times A^* - p\nabla(\nabla\cdot A^*) + \frac{1}{\lambda_L^2}A^* - \frac{\Phi_0}{2\pi\lambda_L^2}\nabla\theta = 0 \quad (19)\\ &\nabla\left(-\frac{1}{\mu_0\lambda_L^2}A^* + \frac{\Phi_0}{2\pi\mu_0\lambda_L^2}\nabla\theta\right) = 0 \quad (20)\end{aligned}\right\}, \quad \text{in } \Omega_1$$

$$\nabla\times\nabla\times A^* - p\nabla(\nabla\cdot A^*) = \mu_0 J - \nabla\times B_Q, \qquad \text{in } \Omega_2 \qquad (21)$$

$$\left.\begin{aligned} &n\times A^* = n\times A = 0 \quad (22)\\ &p\nabla\cdot A^* = 0 \quad (23)\end{aligned}\right\}, \quad \text{on } \Gamma_B$$

$$\left.\begin{aligned} &\nabla\times A^*\times n = \mu_0 H_{ext} - B_Q\times n \quad (24)\\ &n\cdot A^* = 0 \quad (25)\end{aligned}\right\}, \quad \text{on } \Gamma_H$$

$$\left.\begin{aligned} &A_1^* = A_2^* \quad (26)\\ &\nabla\times A_1^*\times n_1 + (\nabla\times A_2^* + B_Q)\times n_2 = 0 \quad (27)\\ &p_1\nabla\cdot A_1^* - p_2\nabla\cdot A_2^* = 0 \quad (28)\\ &n\cdot\left(-\frac{1}{\mu_0\lambda_L^2}A^* + \frac{\Phi_0}{2\pi\mu_0\lambda_L^2}\nabla\theta\right) = 0 \quad (29)\end{aligned}\right\}, \quad \text{on } \Gamma_{12}$$

$-p\nabla(\nabla\cdot A^*)$, and by adding conditions (22) and (25) on Γ_B and Γ_H. The factor p is a constant which is chosen empirically [6]. We simply get the uniqueness of θ by fixing its value at one point in Ω_1.

The Galerkin weighted residual method (see [7] and [8]) is used to discretize (16), (19), (20), and (21). Consequently, considering v_i, w_i, and W_i as weighting factors, the weak form of these equations are

$$\int_{\Omega_2}[\nabla v_i\cdot\nabla\Psi]\,d\Omega = \int_{S_a}[v_i B_{QS}]\,dS \qquad (30)$$

$$\int_{\Omega_1}[\nabla\times W_i\cdot\nabla\times A^* + p\nabla\cdot W_i\nabla\cdot A^* + \frac{1}{\lambda_L^2}W_i\cdot A^* - \frac{\Phi_0}{2\pi\lambda_L^2}W_i\cdot\nabla\theta\,d\Omega = 0 \qquad (31)$$

$$\int_{\Omega_1}\left[-\frac{1}{\mu_0\lambda_L^2}\nabla w_i\cdot A^* + \frac{\Phi_0}{2\pi\mu_0\lambda_L^2}\nabla w_i\cdot\nabla\theta\right]d\Omega = 0 \qquad (32)$$

$$\int_{\Omega_2}[\nabla\times W_i\cdot\nabla\times A^* + p\nabla\cdot W_i\nabla\cdot A^*]\,d\Omega = -\int_{\Omega_2}[\nabla\times W_i\cdot B_Q]\,d\Omega + \int_{\Gamma_H}W_i\cdot[\mu_0 H_{ext}]\,d\Gamma. \qquad (33)$$

The approximation of Ψ which is

$$\Psi = \sum_{j=1}^{Nn} v_j\Psi_j,$$

give a first symmetrical and well-conditionned linear system of N_n equations with N_n unknowns

$$\sum_{j=1}^{Nn}\left[\int_{\Omega_2}[\nabla v_i\cdot\nabla v_j]\,d\Omega\right][\Psi_j] = \left[\int_{S_a}[v_i B_{QS}]\,dS\right].$$

Writing $A*$ and θ by their approximated form

$$A^* = \sum_{j=1}^{Nn} W_j A_j^*$$

and

$$\theta = \sum_{j=1}^{nn} w_j\theta_j$$

in (31)–(33) gives the second linear system

$$\sum_{j=1}^{Nn}\left[\int_{\Omega_1}\left[\nabla\times W_i\cdot\nabla\times W_j + p\nabla\cdot W_i\nabla\cdot W_j + \frac{1}{\lambda_L^2}W_i\cdot W_j\right]d\Omega\right][A_j^*] + \sum_{j=1}^{Nn}\left[\int_{\Omega_1}\left[-\frac{\Phi_0}{2\pi\lambda_L^2}W_i\cdot\nabla w_j\right]d\Omega\right][\theta_j] = 0 \qquad (35)$$

$$\sum_{j=1}^{Nn}\left[\int_{\Omega_1}\left[-\frac{1}{\mu_0\lambda_L^2}\nabla w_i\cdot W_j\right]d\Omega\right][A_j^*] + \sum_{j=1}^{Nn}\left[\int_{\Omega_1}\left[\frac{\Phi_0}{2\pi\mu_0\lambda_L^2}\nabla w_i\cdot\nabla w_j\right]d\Omega\right][\theta_j] = 0 \qquad (36)$$

$$\sum_{j=1}^{Nn}\left[\int_{\Omega_2}[\nabla\times W_i\cdot\nabla\times W_j + p\nabla\cdot W_i\nabla\cdot W_j]\,d\Omega\right][A_j^*] = -\sum_{j=1}^{Nn}\left[\int_{\Omega_2}[\nabla\times W_i\cdot\nabla v_j]\,d\Omega +\right][\Psi_j] + \left[\int_{\Gamma_H}[W_i\cdot(\mu_0 H_{est})\,d\Gamma\right]. \qquad (37)$$

This system of $4N_n$ equations with $4N_n$ unknowns becomes symmetrical and well-conditioned when (36) is multiplied by

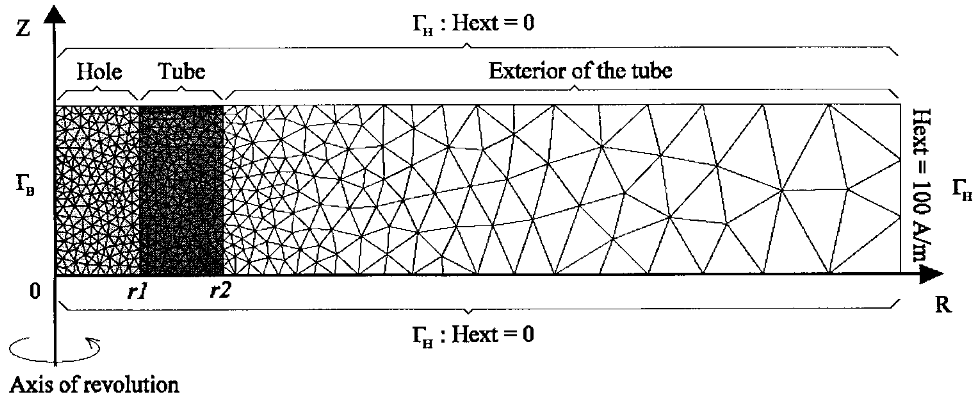

Fig. 2. Meshing of the superconducting tube. The interior and exterior radius of the tube, respectively $r1$ and $r2$, are equal to 1 and 2 μm.

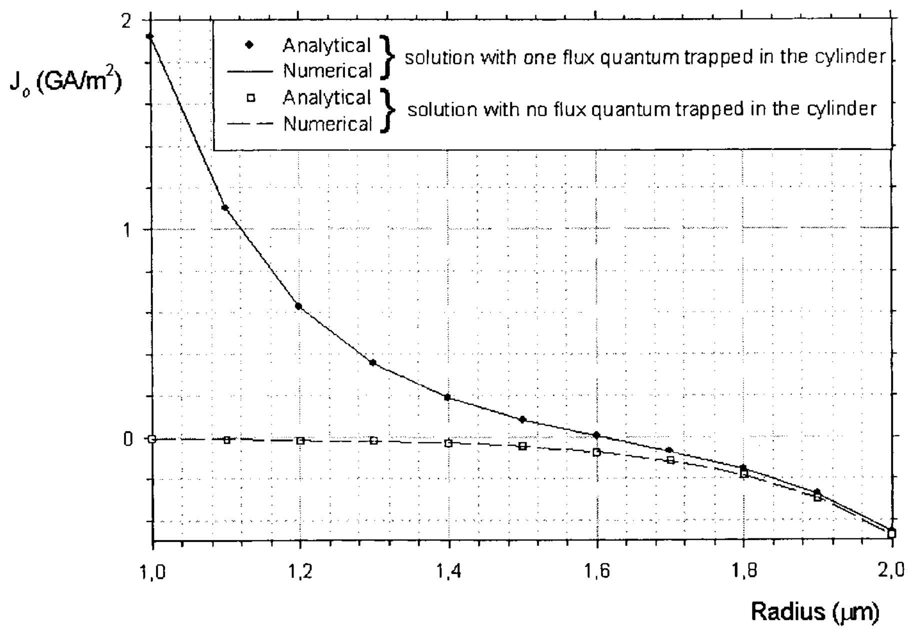

Fig. 3. Analytical [8] and numerical orthoradial supercurrent density distribution in a superconducting tube submitted after the transition to a magnetic field of 100 A$\cdot$m^{-1} along its axis ($\lambda_L = 0.2$ μm). In the first case, a single flux quantum has been trapped in the cylinder during the normal to superconducting transition whereas in the second case none has been. The interior and exterior radius of the tube are, respectively, equal to 1 and 2μm.

$\mu_0\lambda_L$, when the variable change $\Theta = (\Phi_0/2\pi\lambda_L)\theta$ is done and when p is chosen equal to unity [1].

We see that these two systems are weakly coupled so that we can solve separately Ψ with (34) and use this solution in the other system to get A^* and θ.

IV. Numerical Tests

In this section, numerical results obtained with our new formulation will be confronted to analytical results. Two different test configurations with multiply connected superconductors have been chosen.

The first one considers an infinite superconducting tube whose interior and exterior radius, respectively r_1 and r_2, are equal to 1 and 2 μm. We examine two different cases. In the first one, we suppose that a single flux quantum has been trapped at the superconducting transition, so that we have taken B_{QS} constant and equal to $\Phi_0/\pi r_1^2$ in a circular section of the hole. In the second case, no flux quantum has been trapped in the cylinder. After the transition the tube is submitted to an external magnetic field $H = 100$ A$\cdot$m^{-1} parallel to its axis. The problem is treated in a plane with second-order triangle elements. The region where the numerical calculation was done is presented in Fig. 2. The finite-element meshing and the boundaries conditions are also given. The region is discretized into 966 elements which leads to a meshing containing 2042 nodes. The computation has been carried out using a SUN Spark 10 workstation with 256Mo of RAM. The CPU time needed for the solution was 30 s. The London penetration depth is equal to 0.2 μm. The analytical results given by Ginzburg [9] are compared with our results in Fig. 3. We see that the two solutions match very well.

The second test configuration considers a single infinite vortex surrounded by an unbounded superconducting region with $\lambda_L = 0.2$ μm. The vortex is supposed completely isolated and is modeled by a cylindrical normal core of radius equal to the coherence length ξ. For calculation, ξ is fixed to 0.02 μm.

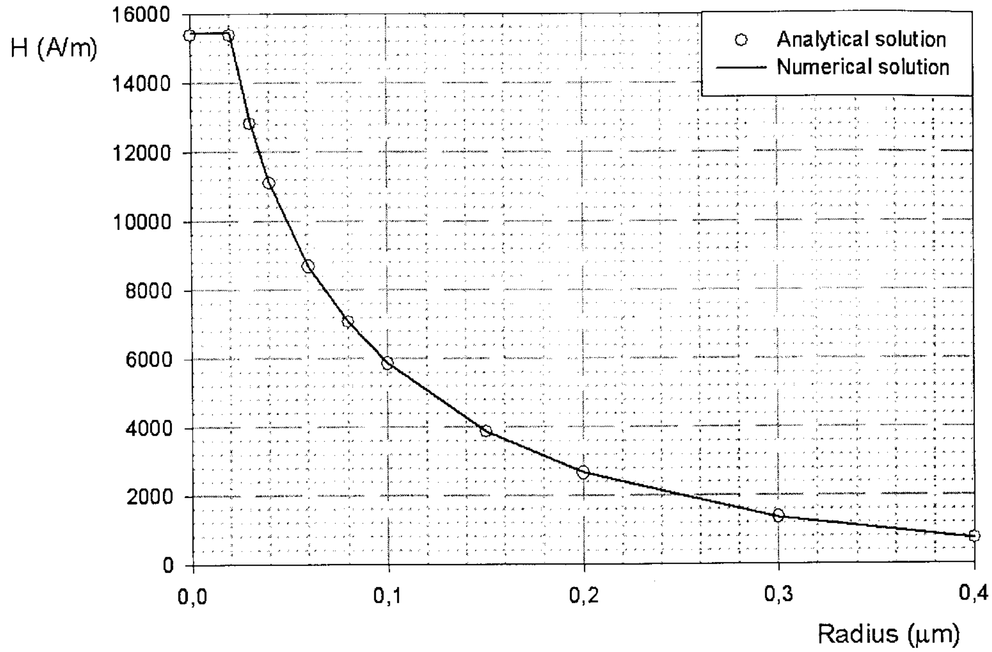

Fig. 4. Analytical [9] and numerical magnetic flux density parallel to the axis of an isolated vortex. The calculation is done in the vicinity of the vortex ($\lambda_L = 0.2$ μm, $\xi = 0.02$ μm).

Of course, the fluxoid is equal to Φ_0, thus we have chosen B_Q equal to $\Phi_0/\pi\xi^2$ in a circular section of the core. A two-dimensional (2-D) meshing with second-order triangle elements is used. This meshing is quite similar to the previous one and leads to computational time of the same order of magnitude. Fig. 4 shows that the analytical formula given in [10] fits very well our numerical solution.

The availability of analytical references concerning structures with axial symmetry has motivated our choice of test configurations. Thus the calculations previously done are of 2-D nature.

Simulating three-dimensional (3-D) thin-film devices such as SQUID is rather difficult as the ratio between thickness and lateral dimensions is large. Indeed, for numerical purposes we must avoid using flat elements. Therefore, even with a single layer of elements in the film, the number of elements required for discretizing these devices is huge. The maximum number of tetrahedral elements which can be used with our workstation is roughly equal to 30 000. With this limitation we can simulate square thin film of approximately $50 \times 50 \times 0.15$ μm, which is far from our expectations. One way to simulate larger superconducting region would be to develop shell elements in order to suppress the discretization of the thickness of the film [11].

V. Conclusion

We have given in this paper a 3-D finite-element formulation for calculating Meissner current in multiply connected superconductors. The fluxoid quantization condition has been taken into account as simply as possible thanks to a relevant variable change.

Numerical solutions given by our method have been confronted to analytical solutions with success. Our method gives a tool to evaluate and optimize superconducting devices (SQUID, Josephson Fraunhofer magnetometer, vortex flux transistor, $\ldots$), whatever the trapped flux.

Nevertheless, the computational means needed for the description of large size devices (typically 300×300 μm) are too important. Further work is in progress to save computational means.

[1] C. Cordier, S Flament, and C. Dubuc, ‘‘A 3D finite element formulation for calculating meissner currents in superconductors,’’ *IEEE Trans. Appl. Superconduct.*, vol. 9, pp. 2–6, Mar. 1999.
[2] P. G. De Gennes, *Superconductivity of Metals and Alloys*. New York: Benjamin, 1966.
[3] A. C. Roses-Innes, *Introduction to Superconductivity*, 2nd ed. New York: Pergamon, 1978.
[4] T. Van Duzer and C. W. Turner, *Principle of Superconductive Devices and Circuits*. New York: Edward Arnold, 1982.
[5] T. P. Orlando, K. A. Delin, *Foundations of Applied Superconductivity*. Reading, MA: Addison-Wesley, 1991, pp. 79–80.
[6] J. L .Coulomb, Ph.D. dissertation, INP, Grenoble, France, 1981.
[7] O. C. Zienkiewicz, *The Finite Element Method*, 3rd ed. New York: McGraw-Hill, 1977.
[8] G. Dhatt and G. Touzot, *Une prsentation de la Mthode des lments Finis*,’’ 2nd ed. Paris, France: Maloine SA, 1984.
[9] V. L. Ginzburg, ‘‘Magnetic flux quantization in a superconducting cylinder,’’ *Sov. Phys.–JETP*, vol 15, no. 1, pp. 207–209, July 1962.
[10] M. Tinkham, *Introduction to Superconductivity*,’’ 2nd ed. New York: McGraw-Hill, 1996, pp. 151–152.
[11] C. Guerin, G. Tanneau, G. Meunier, P. Labie, T. Ngnegueu, and M. Sacotte, ‘‘A Shell element for computing 3D Eddy currents—Application to transformers,’’ *IEEE Trans. Magn.*, vol. 31, pp. 1360–1363, May 1995.

Christophe Cordier received the Engineer degree from the ISMRA-ENSI de Caen in 1997.

He is currently pursuing the Ph.D. degree in electrical engineering at the Universit de Caen. His research focuses on the study and modeling of superconducting devices.

Stéphane Flament received the Engineer degree from the ISMRA-ENSI de Caen in 1991, and the PhD degree from the Universit de Caen in 1994, all in electrical engineering.

He is a Lecturer at the ISMRA in the Electrical Engineering Department. His research domain deals essentially with high Tc low noise superconducting magnetometers, including device modeling and default analysis.

Christian Dubuc received the Engineer degree from the ISMRA-ENSI, Caen, France, in 1968, and the PhD degree from the Universit of Caen, in 1972, all in electrical engineering.

He spent two years at Philips Components Research Laboratory of Caen, working in the area of semiconductors nuclear detectors. After leaving Philips and spending six years at the ISMRA of Caen, he joined the University of Caen in 1978, where he is a Professor in the Departement of Physics and Electrical Engineering. His research interests include superconducting sensors and circuits with an emphasis on high-temperature superconducting devices modeling.